From ubiquitin-proteasomal degradation to CDK1 inactivation: requirements for the first polar body extrusion in mouse oocytes

Yael Pomerantz,[1] Judith Elbaz,[1] Inbal Ben-Eliezer, Yitzhak Reizel, Yael David, Dalia Galiani, Nava Nevo, Ami Navon, and Nava Dekel[2]

Department of Biological Regulation, The Weizmann Institute of Science, Rehovot, Israel

ABSTRACT **Completion of the first meiotic division, manifested by extrusion of the first polar body (PBI), depends on proteasomal degradation of cyclin B1 and securin and the subsequent respective CDK1 inactivation and chromosome segregation. We aimed at identifying the polyubiquitin signal that mediates proteasomal action and at a better characterization of the role of CDK1 inactivation at this stage of meiosis. Microinjections of mutated ubiquitin proteins into mouse oocytes revealed that interference with lysine-11 polyubiquitin chains abrogated chromosome segregation and reduced PBI extrusion by 63% as compared to WT ubiquitin-injected controls. Inactivation of CDK1 in oocytes arrested at first metaphase by a proteasome inhibitor fully rescued PBI extrusion. However, removal of CDK1 inhibition failed to allow progression to the second metaphase, rather, inducing PBI reengulfment in 62% of the oocytes. Inhibition of either PLK1 or MEK1/2 during the first anaphase changed spindle dimensions. The PLK1 inhibitor also blocked PBI emission and prevented RhoA translocation. Our results identified lysine-11 rather than the canonic lysine-48 ubiquitin chains as the degradation signal in oocytes resuming meiosis, further disclosing that CDK1 inactivation is necessary and sufficient for PBI emission. This information significantly contributes to our understanding of faulty chromosome segregation that may lead to aneuploidy.—Pomerantz, Y., Elbaz, J., Ben-Eliezer, I., Reizel, Y., David, Y., Galiani, D., Nevo, N., Navon, A., Dekel, N. From ubiquitin-proteasomal degradation to CDK1 inactivation: requirements for the first polar body extrusion in mouse oocytes. *FASEB J.* 26, 4495–4505 (2012). www.fasebj.org**

Key Words: meiosis · PLK1 · MEK1/2 · chromosome segregation · cell division

MEIOSIS IN OOCYTES IS A protracted process, which includes two asymmetric cell divisions. The first, reductional division, during which the homologous chromosomes segregate, is particularly error prone. Unfaithful first meiotic division may lead to aneuploidy and genetic malformations (1, 2). In mammalian females, meiosis is initiated during embryonic life, during which time pairs of homologous chromosomes undergo recombination and remain attached at the chiasmata. Oocytes arrest prior to birth at the first diplotene and resume their meiotic division at puberty, when, at each reproductive cycle, selected fully grown oocytes respond to the preovulatory surge of luteinizing hormone (LH). Fully grown oocytes will also resume meiosis spontaneously on their isolation from the ovarian follicle (3, 4). Progression to the first metaphase (MI) requires the gradual activation of cyclin-dependent kinase 1 (CDK1), a key regulator of meiosis. Heterodimerization of CDK1 with its regulatory subunit, cyclin B1, followed by dephosphorylation of the kinase, brings about the formation of an active complex, also known as maturation-promoting factor (MPF). An active CDK1 leads to chromosome condensation and the formation of the MI spindle, while its subsequent inactivation, as a result of proteasomal degradation of cyclin B1, is necessary for the metaphase-to-anaphase transition and first polar body (PBI) extrusion (5–7). Notably, the prevention of CDK1 inactivation by proteasome inhibition results in MI arrest, blocking the emission of PBI, the event that represents the completion of the first meiotic division (8–10). Unlike somatic cells, which exit mitosis and enter G_1, in oocytes, CDK1 is reactivated after MI. These oocytes progress immediately to the second metaphase (MII), at which they arrest until fertilization. Another protein subjected to proteasomal degradation at the metaphase-to-anaphase transition is securin, the negative regulator of the

Abbreviations: APC/C, anaphase-promoting complex/cyclosome; CDK1, cyclin-dependent kinase 1; CDK1-I, cyclin-dependent kinase 1 inhibitor; GV, germinal vesicle; MEK1/2, mitogen-activated protein kinase kinase 1/2; MEK-I, mitogen-activated protein kinase kinase 1/2 inhibitor; MI, first metaphase; MII, second metaphase; PBI, first polar body; PFA, paraformaldehyde; PLK1, Polo-like kinase 1; PLK1-I, Polo-like kinase 1 inhibitor; PMSG, pregnant mare serum gonadotropin; Pr-I, proteasome inhibitor; WT, wild type

[1] These authors contributed equally to this work.

[2] Correspondence: Department of Biological Regulation, The Weizmann Institute of Science, Rehovot, Israel. E-mail: nava.dekel@weizmann.ac.il

doi: 10.1096/fj.12-209866

This article includes supplemental data. Please visit *http://www.fasebj.org* to obtain this information.

endopepetidase separase (11–13). Upon securin degradation, separase cleaves a protein complex known as cohesin, which maintains sister chromatid cohesion. The cleavage of cohesion along the chromosomes arms allows the dissolution of the chiasmata and the consequent faithful segregation of homologous chromosomes at anaphase (9, 10, 14–16).

The control over CDK1 inactivation, chromosome segregation, and PBI extrusion is conferred by the ubiquitin-proteasome pathway (UPP). The UPP consists of ubiquitin, an array of E1, E2, and E3 ubiquitin ligases, and the 26S proteasome. The assembly of polyubiquitin chains on substrate proteins is a well-established post-translational modification that mediates various cellular signals, including protein degradation. The type of signal depends on the specific lysine residue by which the chain is assembled (17). Prior to cell division, a specific E3 ubiquitin ligase, the anaphase-promoting complex/cyclosome (APC/C) tags its protein substrates, cyclin B1 and securin, with polyubiquitin chains, which are recognized by the 26S proteasome (reviewed in ref. 12). Lysine-48-linked polyubiquitin chains are the well-established signal for proteasomal degradation (17). However, recent studies have shown that lysine-11 chains enable the degradation of mitotic substrates (18–21). It is currently unknown which chain topology is dominant in oocytes during PBI extrusion. The degradation of substrates by the APC/C is stalled throughout spindle assembly, to prevent premature anaphase and avoid segregation errors (22, 23). An array of proteins, collectively referred to as the spindle assembly checkpoint (SAC), provides a surveillance mechanism that inhibits APC/C activity, until all chromosome kinetochores are properly bound to the spindle (24–26).

The key kinase regulating meiosis is CDK1; however, several other kinases, such as polo-like kinase 1 (PLK1) and mitogen-activated protein kinase kinase 1/2 (MEK1/2) play multiple roles in this process (27, 28). While MEK1/2 is known to partake in the MI spindle assembly and relocation (29–33) and to be essential for the maintenance of the second meiotic arrest (34–37), its possible role during PBI emission is currently undercharacterized. Early meiotic roles for PLK1, such as its involvement in CDK1 autoamplification and in spindle formation, were demonstrated (38, 39). During mitotic anaphase PLK1 was shown to regulate cleavage furrow initiation (40–42); however, this role was never evaluated during meiosis. Since both PLK1 and MEK1/2 play crucial roles in early meiosis, experimental down-regulation of these kinases did not allow the identification of their function at later stages of the meiotic division. Small-molecule inhibitors for PLK1 and MEK1/2 do allow the precise temporal control over the inactivation of these kinases (32, 43, 44) and can therefore facilitate timely analysis of their function during PBI emission.

In the current study, we designed a set of experiments directed at analyzing the ubiquitin chain topology that provides the degradation signal leading to PBI formation. We further aimed to distinguish the specific role of cyclin B1 degradation and the subsequent CDK1 inactivation from that of securin. We also examined the necessity of protein degradation for the progression of meiosis to MII and, in addition, explored the roles of PLK1 and MEK1/2 during the first anaphase.

MATERIALS AND METHODS

Reagents

Leibovitz's L-15 tissue culture medium and FBS were purchased from Biological Industries (Kibbutz Beit Hemeek, Israel). Antibiotics were obtained from Bio-Lab (Jerusalem, Israel), and PBS was obtained from Life Technologies (Invitrogen, Carlsbad, CA, USA). Pregnant mare serum gonadotropin (PMSG) was supplied by Bionieche Animal Health (Brisbane, QLD, Australia); flavopiridol, UO126, and MG132 were purchased from Alexis Biochemicals (San Diego, CA, USA); and BI2536 was from JS Research Chemical Trading (Wedel, Germany). Paraformaldehyde (PFA), Hoechst DNA dye, anti-α-tubulin, and fluorescein isothiocyanate-conjugated anti-α-tubulin monoclonal antibodies were purchased from Sigma-Aldrich Corp. (St. Louis, MO, USA). Anti-RhoA was from Santa Cruz Biotechnology (Santa Cruz, CA, USA). Secondary antibodies and Cy3-conjugated goat anti-mouse F(ab)′ IgG antibodies were from Jackson Laboratory (Bar Harbor, ME, USA). Velcade was a gift from Dr. Ami Navon (Weizmann Institute of Science).

Animals

Female mice (C57BL/6, 24–25 d old) were purchased from Harlan Laboratories (Rehovot, Israel) and handled according to U.S. National Institutes of Health and Weizmann Institute guidelines for management of laboratory animals. The animals were housed in a light- and temperature-controlled room, with food and water provided *ad libitum*.

Oocyte collection and culture

Mice were sacrificed 48 h after subcutaneous injection with 5 IU PMSG for induction of follicular development. The ovaries were removed and placed in L-15 medium, supplemented with 5% FBS, penicillin (100 IU/ml), and streptomycin (100 mg/ml). Large antral follicles were punctured under a stereoscopic microscope (SMZ1500; Nikon, Tokyo, Japan) to release the oocytes. Denuded fully grown oocytes were incubated at 37°C in a humidified incubator. Mouse oocytes released from the ovary contained a visible germinal vesicle (GV), indicating that they were arrested at the prophase of the first meiosis. Upon their isolation, oocytes resume meiosis spontaneously; meiotic progression was monitored in all experiments. For meiotic arrest, oocytes were incubated in a proteasome inhibitor. To minimize indirect effects of the inhibitors, all experiments were repeated with either MG132, a widely used, highly potent proteasome inhibitor, or with the next-generation, highly specific Velcade (bortezomib; PS341; refs. 45, 46).

Protein microinjection

Freshly isolated oocytes separated from their surrounding cumulus cells were transferred to 10-μl drops under paraffin oil, placed under an inverted DIC microscope (Axiovert 35;

Zeiss, Oberkochen, Germany), and microinjected using an InjectMan NI2 micromanipulator and a FemtoJet automated microinjector (Eppendorf, Hamburg, Germany). Micropipettes were pulled manually using an M-97 Flaming/Brown micropipette puller (Sutter Instruments, Novato, CA, USA). Recombinant ubiquitin mutants were prepared as described previously (47) and used at a concentration of 5 mg/ml.

Protein extraction and Western blot analysis

Oocytes (50/group) were collected, washed in PBS, lysed in sample buffer (2% β-mercaptoethanol; 2% sodium dodecyl sulfate; 50 mM Tris-HCl, pH 6.8; 10% glycerol; and 0.01% bromophenol blue) and boiled. Samples were loaded onto 10% SDS-PAGE. After electrophoretic separation, proteins were transferred to a nitrocellulose membrane (Whatman, Dessel, Germany), blocked for 30 min [5% nonfat dry milk and 0.05% Tween in Tris-buffered saline (TBST)], and incubated with anti-securin or anti-tubulin primary antibodies (overnight, 4°C). Membranes were then incubated with secondary anti-mouse horseradish peroxidase-conjugated antibodies for 1 h and exposed to enhanced chemiluminescence reagent (Amersham, Little Chalfont, UK).

Immunofluorescence and microscope image acquisition

The oocytes were fixed in PFA (3.6% in PBS) for 15 min, washed in PBS, and kept in GB-PBS (PBS containing 10 mg/ml BSA and 10 mM glycine, pH 7.4). Permeabilization was performed in 0.1% Triton X-100 in PBS for 15 min, followed by 1 h blocking in GB-PBS. For DNA and tubulin staining, oocytes were incubated with fluorescein isothiocyanate-conjugated tubulin antibodies (1:100) and Hoechst (5 μg/ml) for 1 h. RhoA staining and mounting in Vectashield (Vector Laboratories, Burlingame, CA, USA) were performed as described previously (48).

The oocytes were visualized using an LSM710 confocal microscope (Zeiss), with an EC Plan-Neofluar ×40/1.30 oil DIC m27 lens. ZEN Light 2009 software (Zeiss) was used for image analysis and processing. For live imaging, oocytes were incubated in Hoechst (1 μg/ml) for 1h. Time-lapse images were acquired using a DeltaVision microscope equipped with ×20/0.75 UPlanSApo, ∞/0.17/FN26.5 lens, and a humidified chamber (Applied Precision, Issaquah, WA, USA). Movies and still images were generated using the softWoRx suite (Applied Precision).

Statistical analysis

Statistical analysis was performed using GraphPad Prism software (GraphPad, San Diego, CA, USA). All experiments were repeated ≥3 times. Results presented as percentages of total were corrected by $y = -\arcsin y^{1/2}$ transformation, prior to the statistical test. Data with normal distribution were analyzed using 1-way ANOVA, followed by Tukey's multiple comparison test, to determine differences between group averages. Data that did not distribute normally were analyzed by Kruskal-Wallis test followed by Dunn's multiple-comparison test, to compare group medians.

RESULTS

Formation of ubiquitin chains is necessary for PBI extrusion in oocytes

It has been previously shown that perturbation of the proteasome effectively blocks PBI emission (8–10). To determine whether polyubiquitination is involved in the formation of PBI, mouse oocytes were microinjected with a ubiquitin mutant in which all lysines were replaced by arginines (0K), designed to block any chain elongation (47). The injected oocytes were incubated in a suboptimal dose of a proteasome inhibitor (Pr-I). This dose did not affect PBI extrusion in noninjected oocytes (65% as compared to 60% with the inhibitor; $P>0.05$; **Fig. 1*A***); however, it enabled a better detection of the effect of the mutant proteins, which was otherwise transient (unpublished results). The 0K ubiquitin mutant microinjected into oocytes blocked PBI extrusion significantly, as compared to oocytes injected with a wild-type (WT) ubiquitin protein (34 and 63%, respectively; $P<0.001$). The injection of the WT ubiquitin slightly increased the fraction of oocytes extruding PBI as compared to those injected by buffer (51%), suggesting that the injected protein made a meaningful addition to the endogenous pool present in the oocytes.

To identify the topology of the polyubiquitin chains that lead to the formation of PBI, oocytes were microinjected with purified ubiquitin proteins. These proteins were mutated at a single lysine residue (K11, K63, or K48), designed to block the elongation of the corresponding chain topologies in a dominant-negative manner. The ubiquitin-mutant groups were compared to 0K and, as a positive control, to WT ubiquitin-injected oocytes. The K11R injection resulted in a significant reduction in PBI extrusion, as compared to the WT ubiquitin microinjection (23 *vs.* 63%, respectively; $P<0.0001$; Fig. 1*A*). Interestingly, there was no statistical difference between the effect of K11R and 0K injection on PBI extrusion (23 and 34%, respectively; $P>0.05$). In contrast, K48R injection allowed the formation of PBI in 46% of the oocytes, an effect that was not significantly different from that of the WT ubiquitin injection (63%) and equivalent to that obtained on buffer injection (51%). Microinjection of the K63R mutant resulted in a similarly insignificant effect on PBI extrusion (44%).

We further studied the effect of either K11R or K48R on chromosome segregation. Oocytes microinjected with K11R or K48R ubiquitin mutants were incubated in an inhibitor-free medium for 12 h, the time required for PBI extrusion. At this point, oocytes were fixed, stained, and evaluated for spindle and chromosomal status. We determined that a significantly higher percentage of oocytes injected with K11R ubiquitin exhibited chromosome missegregation, as compared to K48R-injected oocytes (35.7% as compared to 4.3%, respectively; $P=0.001$, Fisher's exact test; Fig. 1*B–D*). Taken together, our results suggest that K11 and not K48 polyubiquitin chains are predominant in mediating PBI extrusion.

CDK1 inactivation induces PBI extrusion under conditions of proteasomal inhibition

To distinguish between the role of cyclin B1 and that of securin degradation, we examined whether, under con-

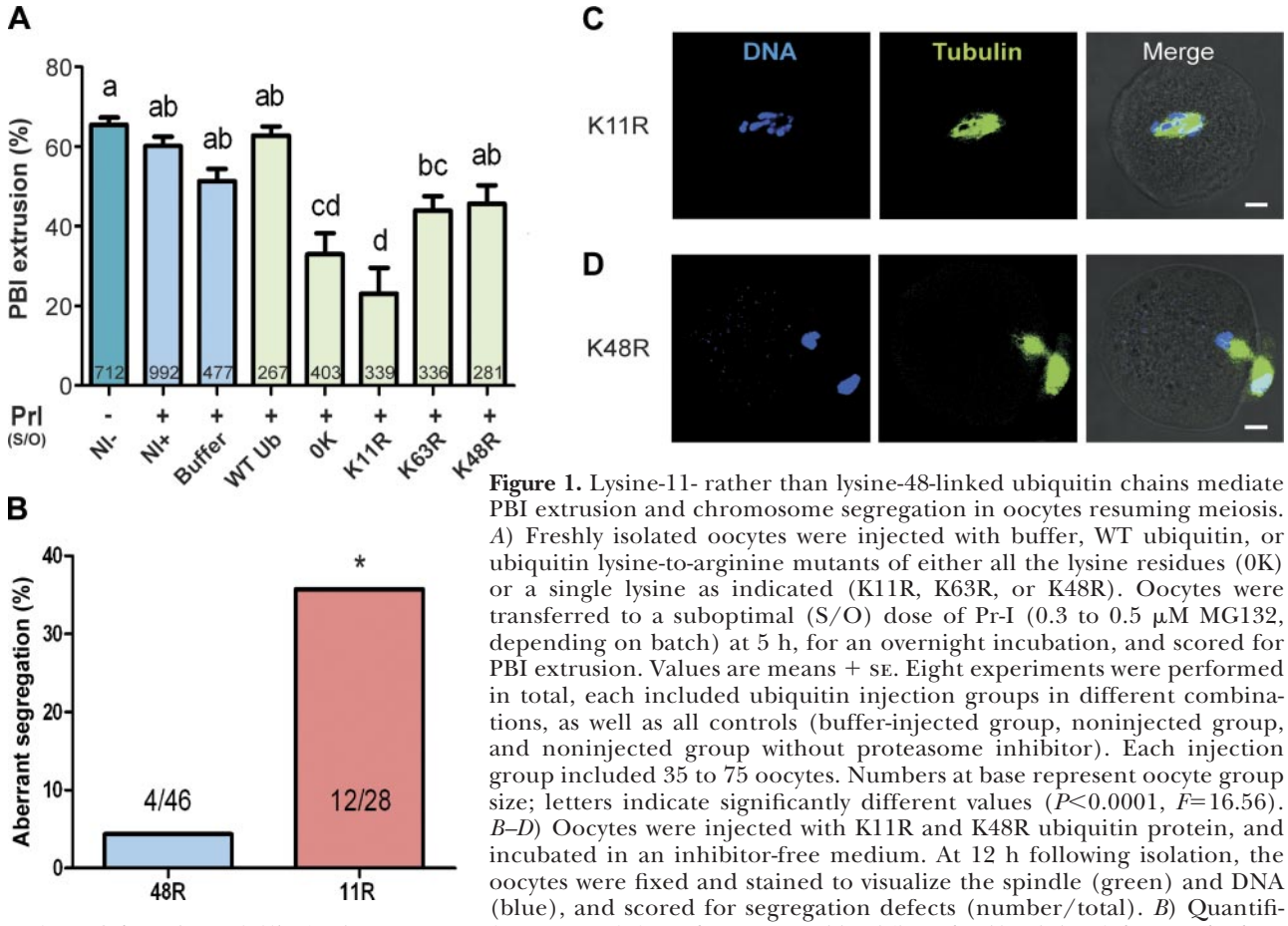

Figure 1. Lysine-11- rather than lysine-48-linked ubiquitin chains mediate PBI extrusion and chromosome segregation in oocytes resuming meiosis. *A*) Freshly isolated oocytes were injected with buffer, WT ubiquitin, or ubiquitin lysine-to-arginine mutants of either all the lysine residues (0K) or a single lysine as indicated (K11R, K63R, or K48R). Oocytes were transferred to a suboptimal (S/O) dose of Pr-I (0.3 to 0.5 μM MG132, depending on batch) at 5 h, for an overnight incubation, and scored for PBI extrusion. Values are means + SE. Eight experiments were performed in total, each included ubiquitin injection groups in different combinations, as well as all controls (buffer-injected group, noninjected group, and noninjected group without proteasome inhibitor). Each injection group included 35 to 75 oocytes. Numbers at base represent oocyte group size; letters indicate significantly different values ($P<0.0001$, $F=16.56$). *B–D*) Oocytes were injected with K11R and K48R ubiquitin protein, and incubated in an inhibitor-free medium. At 12 h following isolation, the oocytes were fixed and stained to visualize the spindle (green) and DNA (blue), and scored for segregation defects (number/total). *B*) Quantification of data. $*P < 0.05$. *C, D*) Representative mutant-injected oocytes: K11R (*C*) and K48R (*D*). Right panels show merges with transmitted light. Scale bars = 10 μm.

ditions of global proteasomal inhibition, the sole inactivation of CDK1 is sufficient to rescue PBI formation. For this purpose, isolated oocytes were treated with different combinations of a Pr-I (either MG132 or Velcade) and a CDK1 inhibitor (CDK1-I; flavopiridol; **Fig. 2*A***). Control oocytes, which were allowed to resume meiosis spontaneously, extruded PBI after ~12 h (Fig. 2*B*, *E* and Supplemental Video S1), whereas Pr-I-treated oocytes remained arrested at MI (Fig. 2*B*, *D*). We found that the addition of CDK1-I on top of the Pr-I rescued PBI extrusion (Fig. 2*B* and Supplemental Video S2). Among oocytes that were supplemented with CDK1-I at 12 h, the fraction of PBI emission was similar to that of untreated controls (56 and 63%, respectively; $P=0.1$).

The CDK1-I in the above experiment was added to the oocytes at 12 h after their isolation from the ovarian follicle, at which time their spindle is fully assembled. To determine whether the stimulation of PBI extrusion by CDK1 inactivation requires a fully assembled spindle, we added the CDK1-I at earlier time points. Inactivation of CDK1 prior to the completion of spindle assembly gave rise to a similar fraction of oocytes emitting PBI (66, 73, and 56% at 7, 9, and 12 h, respectively; $P=0.1$; Fig. 2*C*). As expected, high incidence of chromosome missegregation and lagging chromosomes was observed (40% at 9 h; Fig. 2*C*). Notably, PBI emission following "premature" CDK1 inactivation was also observed in oocytes upon the addition of CDK1-I to oocytes incubated in Pr-I-free medium (75%; Fig. 2*B*).

CDK1 inactivation induces metaphase-to-anaphase transition and chromosome segregation in the presence of an intact securin

To examine their chromosomal configuration, oocytes treated with a combination of Pr-I and CDK1-I, as described previously, were fixed and stained. All oocytes that were incubated with the Pr-I alone for either 12 or 24 h remained arrested at MI, as indicated by their unsegregated chromosomes and nonelongated spindles (Fig. 2*C*, *D*). In contrast, most oocytes exposed to Pr-I and CDK1-I underwent either partial (55%; Fig. 2*C*, *H*) or complete (15%; Fig. 2*C*, *G*) chromosome segregation, while only 22% were arrested at MI (Fig. 2*C*, *F*). Partial segregation was defined when one or more chromosomes migrated to the spindle poles, while the rest of the DNA remained at the equator. These spindles often contained noticeably stretched chromosomes, or chromosomes that were lagging between the equator and the poles (Fig. 2*H*, inset). Surprisingly, chromosome segregation occurred despite the presence of securin (Fig. 2*J*). The assessment of chromosome segregation was done at 12 h, the regular time of PBI extrusion, to exclude a possible "cohesion

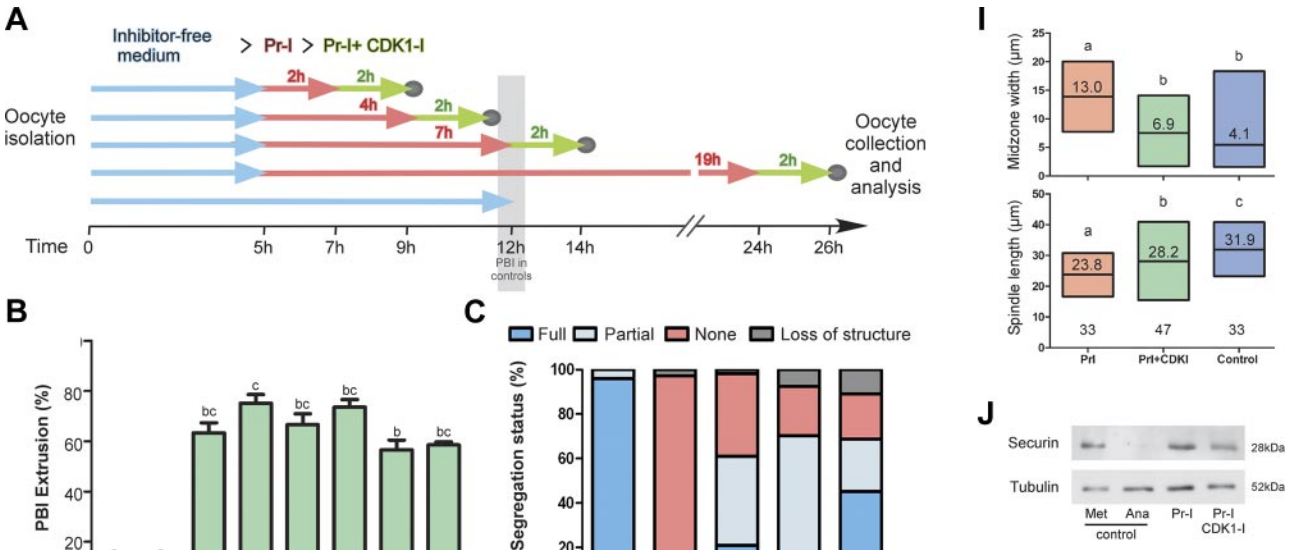

Figure 2. Extrusion of PBI is rescued by CDK1 inactivation regardless of proteasomal inhibition. *A*) Experimental design: oocytes incubated for 5 h in an inhibitor-free medium (blue arrows) were transferred to a medium containing Pr-I (2 μM MG132 or velcade; red arrows) for an additional 2, 3, 5 and 19 h of incubation. Oocytes of each group were further exposed to a CDK1-I (10 μM flavopiridol; green arrows) for 2 h, after which they were collected and monitored for PBI extrusion. Control oocytes were incubated in an inhibitor-free medium (blue arrow) for 12h. *B*) Proportion of PBI extrusion in oocytes treated as detailed in *A*. Bars represent means + SE of ≥3 independent experiments; numbers represent oocyte group size. Letters indicate statistically significant differences ($P<0.0001$). *C–I*) Oocytes were fixed in PFA; spindles (green) and DNA (blue) were stained. *C*) Distribution of chromosome segregation phenotypes. Total number of oocytes in ≥3 different experiments is indicated. *D*) Oocyte treated with Pr-I for 12 h. *E*) Untreated oocyte extruding PBI after 12 h of incubation. *F–H*) Oocytes treated with Pr-I and CDK1-I at 12 h; numbers represent percentages of nonsegregated (*F*), fully segregated (*G*), and partially segregated (*H*) chromosomes. Inset: DNA channel only; arrow marks a stretched chromosome. Scale bars = 10 μm. *I*) Spindle midzone width (top panel) and length (bottom panel) were compared between oocytes arrested at MI by Pr-I (red); oocytes arrested by Pr-I, which extruded PBI in response CDK1-I treatment, presenting either partial or complete chromosome segregation (green); and nontreated oocytes after 12 h (blue). Bars mark minimal to maximal values in each group. Central lines and corresponding numbers represent medians (width) or means (length). Letters indicate significantly different groups (spindle width: $P=0.0008$; spindle length: $P<0.0001$). *J*) Oocytes (50/lane) were subjected to Western blot analysis for securin immunodetection; α-tubulin served as a control. Untreated oocytes were collected at metaphase (Met-8h of incubation) or at anaphase (Ana-12h of incubation); oocytes arrested in MI by Pr-I with or without CDK1-I were collected after 14 h of incubation. CDK1-I was added for the last 2 h of incubation. Blot is representative of 4 independent experiments.

fatigue," a situation in which cohesion may be weakened due to an extended metaphase arrest (49).

The rescue of PBI emission by CDK1-I was further characterized by two additional anaphase hallmarks, the changes in spindle dimensions and the localization of RhoA small GTPase. Spindles of untreated oocytes, measured from pole to pole, elongated at anaphase to reach 31.9 μm (Fig. 2*I*, bottom panel). While Pr-I treatment inhibited this elongation (23.8 μm), the addition of CDK1-I to these oocytes induced spindle elongation (28.2 μm; $P<0.001$ *vs.* Pr-I treated oocytes). Midzone width, measured at the central part of the spindle, contracts during anaphase to reach an average of 4.1 μm (Fig. 2*I*, top panel). Midzone contraction was blocked by Pr-I treatment (13 μm) and restored by the addition of CDK1-I (6.9 μm, similarly to untreated oocytes; $P=0.008$). In a previous study, we demonstrated that RhoA accumulates at the midzone during PBI extrusion (48). We show herein that no RhoA was detected in oocytes arrested at MI by Pr-I (see **Fig. 4*E***), whereas a similar pattern of RhoA recruitment was observed in the current study, upon the rescue of PBI formation by CDK1-I (see Fig. 4*D*, top panels).

Cytokinesis is reversible under conditions of proteasome inhibition

The progression of oocytes to MII depends on reactivation of CDK1 (50). We examined whether removal of the CDK1-I will move meiosis forward to MII in our experimental system. For this purpose, we first treated Pr-I-arrested oocytes with CDK1-I. Oocytes that have

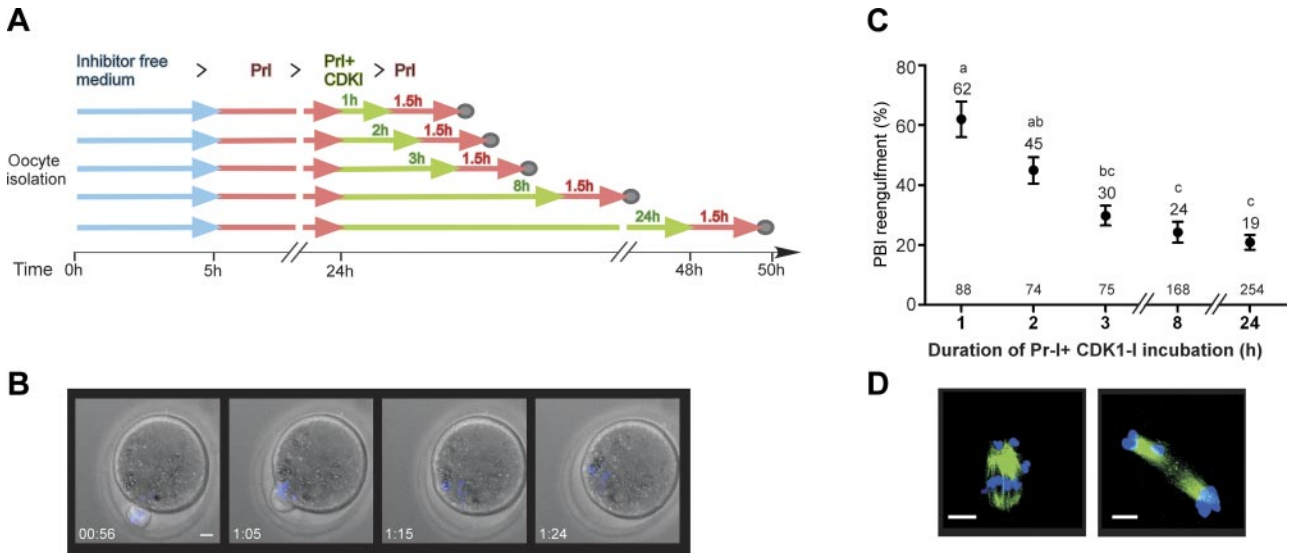

Figure 3. Transient CDK1 inactivation in the absence of proteasomal activity leads to reversal of meiosis. *A*) Experimental design: isolated oocytes incubated in inhibitor-free medium for 5 h (blue arrows) were transferred to a medium containing Pr-I (2 μM MG132; red arrows) after 5 h. After overnight incubation, a CDK1-I (10 μM flavopiridol; green arrows) was added for an additional 1, 2, 3, 8, and 24 h. Oocytes with PBI were then transferred to a Pr-I-containing medium and monitored for PBI after 1.5 h. *B*) Sequential frames from time-lapse microscopy of PBI reengulfment (full film provided in Supplemental Material). An oocyte that was incubated in Pr-I overnight, transferred to Pr-I + CDK1-I for 8 h, and then extruded a PBI was subsequently stained with Hoechst (DNA) and examined upon its transfer to Pr-I. Time (h) after transfer to Pr-I is shown. *C*) Percentage of oocytes exhibiting PBI reengulfment at different CDK1-I incubation periods. Values are means ± SE of ≥3 independent experiments. Numbers at base represent total oocyte group size. Letters indicate significantly different values ($P<0.0001$). *D*) Oocytes that had reengulfed PBI after transfer to Pr-I were fixed and stained for spindle (green) and DNA (blue). Scale bars = 10 μm. $n = 72$.

extruded PBI were selected and transferred to a medium containing Pr-I without CDK1-I, to allow CDK1 reactivation, thus mimicking the transient CDK1 inactivation between the two meiotic divisions (**Fig. 3*A***). We found that under proteasomal inhibition, removal of the CDK1-I did not drive oocytes to MII, but rather induced reversal of cytokinesis, manifested by reengulfment of the extruded PBIs (Fig. 3*B* and Supplemental Video S3). The ability of the oocytes to reverse cytokinesis declined with time; while 62% of the Pr-I treated oocytes reengulfed their PBIs after 1 h exposure to CDK1-I, longer treatments significantly reduced the incidence of PBI reengulfment (Fig. 3*C*). Interestingly, among oocytes that were incubated for 24 h in both Pr-I and CDK1-I, a fraction of 19% still maintained the capacity to reengulf their PBI. Time-lapse microscopy and immunostaining of oocytes fixed after PBI reengulfment revealed that most oocytes, with and without PBI, contained first telophase spindles with fully or partially segregated chromosomes, localized either within the oocyte or between the oocyte and PBI. MII spindles were never observed, indicating failure to proceed to MII (Fig. 3*B, D* and Supplemental Video S3).

Cytokinesis induced by CDK1 inactivation is mediated by PLK1 but not by MEK1/2

To test the possible involvement of PLK1 and MEK1/2 following CDK1 inactivation, we used selective inhibitors (BI2536 and UO126, respectively). Oocytes arrested at MI by an overnight incubation in Pr-I were induced to form PBI by CDK-I, as described above. The addition of PLK1 inhibitor (PLK1-I) concomitantly with the CDK1-I blocked PBI extrusion (8.6%; $P<0.0001$; Fig. 4*A*), whereas MEK1/2 inhibitor (MEK-I) had no effect on this event (53%, *vs.* 52% in the control). Moreover, RhoA enrichment around the midzone was abrogated upon the addition of PLK1-I but not MEK-I (Fig. 4*D*, middle and bottom, panels, respectively), indicating that the PLK1 control of cytokinesis is mediated by RhoA accumulation.

PLK1 and MEK1/2 determine spindle dimensions during anaphase I

We further examined the role of PLK1 and MEK1/2 in determining spindle morphology at anaphase I. As described above, treatment of Pr-I and CDK1-I induced anaphase I, characterized by spindle elongation and midzone contraction (Figs. 2*I* and 4*B*). The addition of PLK1-I prevented the spindle elongation induced by CDK1 inactivation (21.1 μm, *vs.* 24.5 μm in oocytes not supplemented with PLK1-I; $P<0.001$; Fig. 4*C, D*, middle panels). An even more dramatic effect was observed at the spindle midzone, which did not contract but was markedly widened by this treatment, the median width reaching 18.5 μm (Fig. 4*B*), which is more than double the width at anaphase I (9.1 μm; $P<0.0001$), and also significantly wider than MI spindles (13.2 μm; $P<0.01$; Fig. 4*B*; compare Fig. 4*D*, middle panels, and *F–H* to *E*).

Interestingly, while inhibition of MEK1/2 did not interfere with PBI emission, it resulted in a distinct shortening of the anaphase I spindle (14.3 μm, *vs.* 24.5 μm in Pr-I+CDK1-treated oocytes, $P < 0.001$; or 23.7

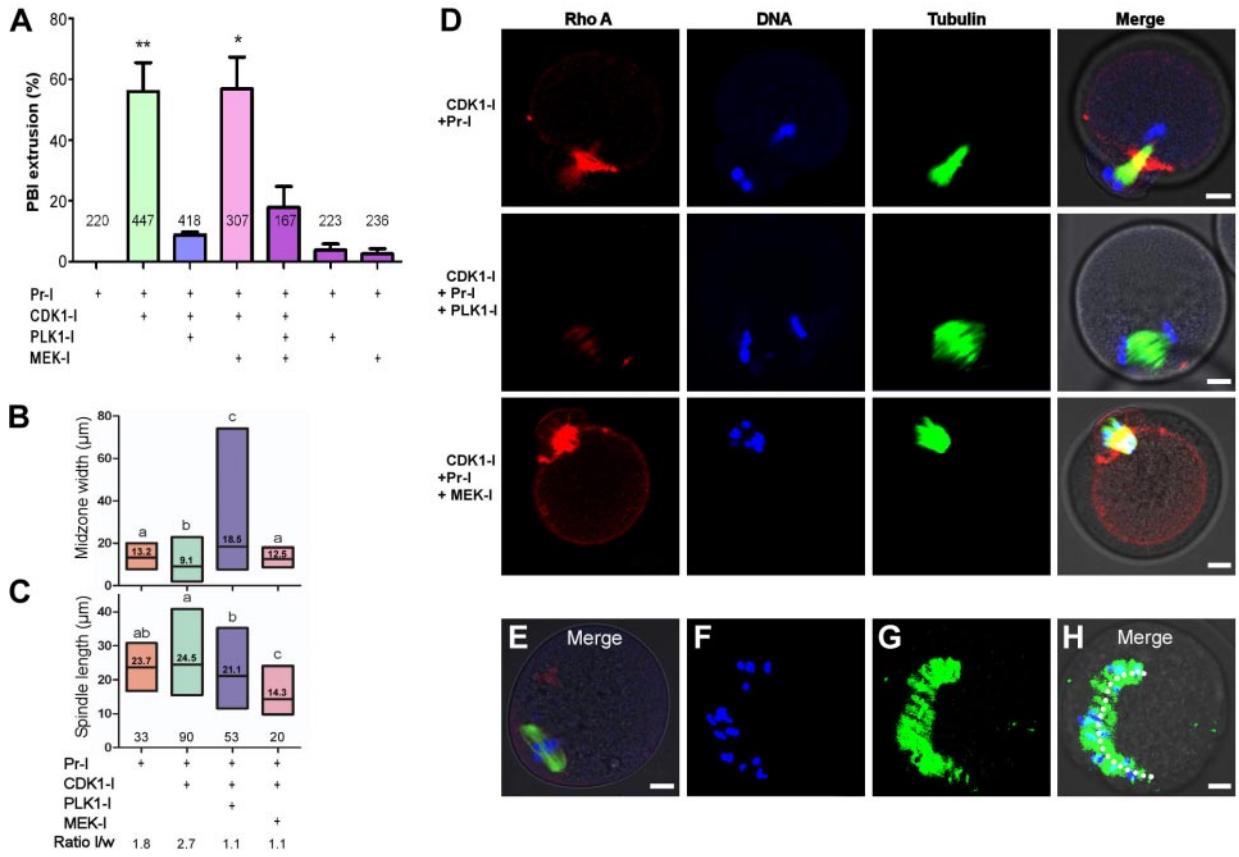

Figure 4. PLK1 mediates cytokinesis, while both PLK1 and MEK1/2 determine anaphase spindle dimensions. *A*) Isolated oocytes transferred after 5 h to Pr-I (2 μM MG132 or velcade, overnight) were transferred to different combinations of Pr-I, CDK1-I, PLK1-I, and MEK-I for 3 h and monitored for PBI extrusion. Values are means + SE of ≥3 independent experiments. $*P < 0.05$, $**P < 0.01$ *vs.* Pr-I. *B–H*) Oocytes treated as in *A* were fixed and stained for spindle and DNA, as well as for RhoA (*D*, *E*). *B*, *C*) Measurements of spindle midzone width (*B*) and spindle pole-to-pole length (*C*). Bars represent minimum-to-maximum values of each group; central lines and numbers represent medians. Numbers at base represent group size, letters indicate significant differences between groups (length: $P<0.001$; width: $P<0.0001$) *D*) Representative images of oocytes treated with Pr-I + CDK1-I (top panels), Pr-I + CDK1-I + PLK1 inhibitor (PLK-I; middle panels), or Pr-I + CDK1-I + MEK-I (bottom panels) were taken under identical exposure settings. *E*) Oocyte arrested in MI after an overnight incubation in Pr-I; merge of DNA, tubulin, and RhoA channels. *F–H*) Oocyte with extreme spindle widening (dotted line depicts spindle width) after treatment with Pr-I + CDK1-I + PLK-I.

μm in MI-arrested oocytes, $P<0.001$; Fig. 4*C*; compare Fig. 4*D*, bottom panels, to *E*). Furthermore, these spindles failed to contract at the midzone ($P<0.01$ *vs.* Pr-I+CDK1-I midzone width; Fig. 4*B*), resulting in "dwarf" spherical spindles with a length/width ratio of 1.1, as compared to 2.7 in Pr-I+CDK-I-treated oocytes (Fig. 4*B*, *D*, bottom panels). It is important to note that both spindle midzone widening by PLK1-I and spindle length shortening by MEK-I did not occur in the absence of the CDK1-I (Supplemental Fig. S1).

DISCUSSION

Ubiquitin chains linked through lysine-11 mediate PBI extrusion

We show herein that formation of polyubiquitin chains is a requirement for meiotic progression. Moreover, we further demonstrate that disruption of K11R- but not K48R-linked ubiquitin chains interfered with PBI extrusion and induced higher incidence of chromosome segregation abnormalities. We thereby provide the first evidence that K11, rather than the canonic K48 chain topology, provides the prevailing signal for proteasomal degradation required for PBI extrusion. These findings are in line with recent *in vitro* studies demonstrating formation of K11 chains by APC/C. In addition, it was shown that disruption of K11 chains affects the degradation of cyclin B1 and securin, further supporting their role in cell division (18–21, 51). Microinjection of the K63R and K48R mutants resulted in mild, statistically insignificant decrease in PBI extrusion. The K48 linkage is a well-established signal for protein degradation in other cellular contexts (17). Surprisingly, our results show that these chains have only minor contributions to proteasomal degradation at this stage of meiosis. The K63 chains, however, are known to function in nonproteolytic pathways, such as a response to DNA double-strand breaks and transmembrane protein

sorting, as well as Toll-like receptor and NF-κB signaling (52–55). The fact that the blockage of this ubiquitin topology has a mild effect on PBI emission raises the need to further investigate these pathways in the first round of meiosis. In addition, the existence of mixed K11, K48, and K63 ubiquitin chains on cellular proteins was previously suggested (21, 56, 57). Branched, heterogeneous chains are not thought to be involved in proteasomal degradation (58). It is possible that K63 chain perturbation has indirectly compromised the oocytes' ability to extrude PBI, reflecting the involvement of this linkage, as heterogeneous or homologous chains, in yet to be explored nonproteolytic cellular functions.

In our system, a suboptimal dose of proteasome inhibitor was added. In its absence, 0K mutant delayed PBI extrusion, but it did not prevent it. This phenomenon may be attributed to the presence of competing endogenous ubiquitin molecules in the oocyte, combined with the activity of deubiquitinating enzymes (DUBs) that constantly remodel ubiquitin chains. The importance of ubiquitin carboxy-terminal hydrolase (UCH)-family DUBs to meiotic progression was recently demonstrated, as their inhibition in oocytes perturbed PBI extrusion, caused MII spindle abnormalities, and prevented fertilization (59, 60). Such substantial activity of DUBs counteracts the effect of the injected chain-blocking mutants, which are removed and replaced by other ubiquitin moieties. The fact that a proteasome inhibitor intensified the effect induced by the ubiquitin mutants further implies that K11 chains function in the degradation pathway. Notably, the mutant-induced chromosome segregation defects observed in this study took place without proteasomal inhibition.

Inactivation of CDK1 is necessary and sufficient for the transition to anaphase and induction of cytokinesis in the first meiotic division

The process of PBI emission is a highly complicated event, strictly regulated to ensure efficient reductional meiotic division, enabling the generation of a haploid nucleus. The present study demonstrates that the inactivation of a single kinase, CDK1, is sufficient for meiotic cytokinesis, indicated by the emission of PBI, as well as for the metaphase-to-anaphase transition, manifested by spindle elongation, midzone contraction, and chromosome segregation. Interestingly, the latter event takes place despite the presence of securin, the negative regulator of separase. Since separase activity is absolutely required for the dissolution of the chiasmata and the subsequent chromosome segregation (10, 16), our data suggest that separase may be activated regardless of the presence of securin, which indicates an additional regulatory mechanism of separase activity. Indeed, it was shown that separase could be inhibited by its phosphorylation and the subsequent binding to the CDK1-cyclin B1 complex (61–64). This interaction is mutually exclusive; thus, at metaphase, each separase molecule is inhibited either by securin or by CDK1-cyclin B1 (61–64). Furthermore, separase binding inhibits CDK1 activity as it was previously shown that prevention of CDK1-separase binding in mouse oocytes blocks PBI extrusion (65). Our findings are complementary to the latter report and may present the other side of the coin: CDK1's contribution to the inhibition of separase. It was previously shown that full, faithful chromosome segregation requires both securin degradation and CDK1 inactivation (61, 63, 64, 66, 67). Indeed, as expected, we observed only partial chromosome segregation under conditions of intact securin. Notwithstanding, our results distinguish the role of CDK1 inactivation in chromosome segregation from that of securin.

Interestingly, somatic cells that were treated with a combination of Pr-I and CDK1-I underwent cytokinesis but not chromosome segregation (68–70). In contrast, we show that oocytes treated similarly undergo PBI extrusion, as well as chromosome segregation, suggesting that CDK1 plays a more dominant role in maintaining meiotic cohesion, as compared to mitosis. Supporting this suggestion, it was previously demonstrated that a certain low dose of an undegradable Δ90 cyclin B1, which maintains low levels of CDK1 activity, was able to inhibit chromosome segregation in oocytes but not in mitotic cells (9, 62). The different effect of CDK1 inactivation on meiotic and mitotic chromosome separation is supported by studies in *Caenorhabdidis elegans*, which showed distinct requirements for anaphase chromosome separation in meiosis, as compared to mitosis (71, 72).

PBI extrusion induced by CDK1 inhibition in the absence of proteasome activity is reversible

Inactivation of CDK1 that enables PBI emission is immediately followed by reactivation of this kinase, which drives meiosis forward, to MII. However, in our study, under conditions of inhibited proteasomal activity, a transient CDK1 inactivation failed to drive meiosis further, but rather resulted in reversal of cytokinesis. This experiment suggests that while CDK1 inactivation brings about the metaphase-to-anaphase transition, protein degradation is required for the forward directionality of meiosis beyond anaphase. Reversal ability was also demonstrated in mitotic cells (68, 73). Nevertheless, in mitosis, the capacity to reverse cell division was conserved for only 1 h, after which it was essentially lost due to the inhibitory phosphorylation of CDK1 by Wee1 and Myt1 kinases (73). In oocytes, CDK1 is not phosphorylated at this stage of meiosis (5), a fact that may explain their extended ability for PBI reengulfment.

PLK1 activity mediates cytokinesis *via* RhoA localization and is required for the contraction of the anaphase I spindle

The use of small-molecule inhibitors in the current study enabled the identification of two PLK1 roles

during a very specific time frame, just prior to PBI extrusion. Previous results from our laboratory showed that the depletion of the guanine nucleotide exchange factor ECT2 from mouse oocytes abolishes RhoA localization, and prevents PBI emission (48). Furthermore, other studies in mitosis indicate that cytokinesis is mediated by PLK1, *via* ECT2-dependent recruitment of RhoA (40, 74). Taken together, these findings strongly imply that the CDK1-PLK1-ECT2-RhoA pathway partakes in PBI emission.

PLK1 inhibition also blocked meiotic spindle elongation and induced midzone widening. Prevention of spindle elongation under similar conditions was previously reported in mitotic cells (44); however, the dramatic widening of the spindles is oocyte-specific. The meiotic, but not mitotic, spindle widening may seed from altered regulation of the female meiotic spindle, which lacks centrioles and centrosomes, but is rather based on microtubule organizing centers (MTOCs) that cluster together and self-organize into a bipolar spindle (reviewed in ref. 75). As the oocyte is much larger than somatic cells, the availability of additional space in the oocyte, which allows the spindle to expand, may also explain this phenomenon. This new role of PLK1 is in line with previous studies in oocytes, which indicated PLK1 association with the spindle poles and chromosomes at metaphase I, followed by translocation to the midzone at anaphase I (39, 76–78).

A novel role for MEK1/2 in the cell cycle: controlling anaphase spindle length

Our results indicate that MEK1/2 inhibition during anaphase I prevented spindle contraction and reduced spindle length. These results are concordant with previous reports that demonstrate ERK1/2 colocalization with the meiotic and mitotic spindles, affecting microtubule dynamics (38, 79, 80). The phenotype of anaphase spindle shrinkage observed by us may appear to be in contradiction to a previously reported phenotype of a small subpopulation of oocytes from mos-depleted ($mos^{-/-}$) mice, in which the MI spindles were enlarged (81). However, the phenotype of the $mos^{-/-}$ oocyte is in fact the result of an event taking place before PBI extrusion, during prometaphase and metaphase. In $mos^{-/-}$ oocytes, MI spindle migration was inhibited and compensated at anaphase I by elongation, resulting in a very large spindle that eventually reached the cortex (29, 82). Our experimental system, unlike the systemic depletion of mos, allowed the addition of the inhibitor to oocytes at a very specific time point, at which the spindles are fully formed and relocated at the cortex. Moreover, spindle shrinkage was anaphase specific, as it required CDK1 inactivation. Therefore, the observed phenotype, in which the spindle shrinks in length, is novel, distinct from the previously reported spindle elongation, and seems to result from aberrant regulation on spindle length once both CDK1 and MEK1/2 activities are missing. Notably, the MI spindle in mouse oocytes is encapsulated by a dynamic structure of actin filaments. This microfilament structure facilitates the spindle translocation and tethering to the cortex (83, 84). As demonstrated in yeast and somatic cells, the actin structure may be linked to spindle microtubules (85, 86) F-actin was shown to affect spindle length in mitotic cells (87). Thus, it is possible that actin filaments are involved in the changes in spindle morphology observed in our study, upon the inhibition of MEK1/2 and PLK1.

CONCLUSIONS

In this study, we investigated the relationship between proteasomal degradation and CDK1 inactivation, two major forces that drive PBI extrusion. Analyzing the signal for proteolysis, we found that the lysine-11 polyubiquitin chain topology is the prevailing signal for PBI extrusion. Our results further demonstrated that inactivation of CDK1 is sufficient for PBI extrusion and that proteasomal degradation is required for the forward progression of the oocyte to the second meiotic division. We found that PLK1 operates downstream of CDK1 inactivation to mediate PBI extrusion, and deciphered the role of PLK1 and MEK1/2 in the control of spindle dimensions. These observations highlight the similarities as well as differences between meiosis and mitosis, and pave the way for future research studying the factors that ensure a faithful completion of meiosis, knowledge that may be applied to prevent genetic malformations and infertility. FJ

The authors thank Dr. Edna Schechtman for statistical analysis. This study was supported by the Dwek Fund for Biomedical Research. N.D. is the incumbent of the Philip M. Klutznick Professorial Chair in Developmental Biology.

REFERENCES

1. Hassold, T., and Hunt, P. (2001) To err (meiotically) is human: the genesis of human aneuploidy. *Nat. Rev. Genetics* **2,** 280–291
2. Hunt, P. A. (1998) The control of mammalian female meiosis: factors that influence chromosome segregation. *J. Assist. Reprod. Genet.* **15,** 246–252
3. Eppig, J. J., and Telfer, E. E. (1993) Isolation and culture of oocytes. *Methods Enzymol.* **225,** 77–84
4. Schultz, R. M., Montgomery, R. R., Ward-Bailey, P. F., and Eppig, J. J. (1983) Regulation of oocyte maturation in the mouse: possible roles of intercellular communication, cAMP, and testosterone. *Dev. Biol.* **95,** 294–304
5. Choi, T., Aoki, F., Mori, M., Yamashita, M., Nagahama, Y., and Kohmoto, K. (1991) Activation of p34cdc2 protein kinase activity in meiotic and mitotic cell cycles in mouse oocytes and embryos. *Development* **113,** 789–795
6. Hashimoto, N., and Kishimoto, T. (1988) Regulation of meiotic metaphase by a cytoplasmic maturation-promoting factor during mouse oocyte maturation. *Dev. Biol.* **126,** 242–252
7. Hampl, A., and Eppig, J. J. (1995) Analysis of the mechanism(s) of metaphase I arrest in maturing mouse oocytes. *Development* **121,** 925–933
8. Josefsberg, L. B., Galiani, D., Dantes, A., Amsterdam, A., and Dekel, N. (2000) The proteasome is involved in the first metaphase-to-anaphase transition of meiosis in rat oocytes. *Biol. Reprod.* **62,** 1270–1277
9. Herbert, M., Levasseur, M., Homer, H., Yallop, K., Murdoch, A., and McDougall, A. (2003) Homologue disjunction in mouse

oocytes requires proteolysis of securin and cyclin B1. *Nat. Cell Biol.* **5,** 1023–1025
10. Terret, M. E., Wassmann, K., Waizenegger, I., Maro, B., Peters, J. M., and Verlhac, M. H. (2003) The meiosis I-to-meiosis II transition in mouse oocytes requires separase activity. *Curr. Biol.* **13,** 1797–1802
11. Holt, J. E., and Jones, K. T. (2009) Control of homologous chromosome division in the mammalian oocyte. *Mol. Hum. Reprod.* **15,** 139–147
12. Jones, K. T. (2011) Anaphase-promoting complex control in female mouse meiosis. *Results Probl. Cell Differ.* **53,** 343–363
13. Hagting, A., Den Elzen, N., Vodermaier, H. C., Waizenegger, I. C., Peters, J. M., and Pines, J. (2002) Human securin proteolysis is controlled by the spindle checkpoint and reveals when the APC/C switches from activation by Cdc20 to Cdh1. *J. Cell Biol.* **157,** 1125–1137
14. Zou, H., McGarry, T. J., Bernal, T., and Kirschner, M. W. (1999) Identification of a vertebrate sister-chromatid separation inhibitor involved in transformation and tumorigenesis. *Science* **285,** 418–422
15. Kudo, N. R., Anger, M., Peters, A. H., Stemmann, O., Theussl, H. C., Helmhart, W., Kudo, H., Heyting, C., and Nasmyth, K. (2009) Role of cleavage by separase of the Rec8 kleisin subunit of cohesin during mammalian meiosis I. *J. Cell. Sci.* **122,** 2686–2698
16. Kudo, N. R., Wassmann, K., Anger, M., Schuh, M., Wirth, K. G., Xu, H., Helmhart, W., Kudo, H., McKay, M., Maro, B., Ellenberg, J., de Boer, P., and Nasmyth, K. (2006) Resolution of chiasmata in oocytes requires separase-mediated proteolysis. *Cell* **126,** 135–146
17. Hershko, A., and Ciechanover, A. (1998) The ubiquitin system. *Annu. Rev. Biochem.* **67,** 425–479
18. Garnett, M. J., Mansfeld, J., Godwin, C., Matsusaka, T., Wu, J., Russell, P., Pines, J., and Venkitaraman, A. R. (2009) UBE2S elongates ubiquitin chains on APC/C substrates to promote mitotic exit. *Nat. Cell Biol.* **11,** 1363–1369
19. Wu, T., Merbl, Y., Huo, Y., Gallop, J. L., Tzur, A., and Kirschner, M. W. (2010) UBE2S drives elongation of K11-linked ubiquitin chains by the anaphase-promoting complex. *Proc. Natl. Acad. Sci. U. S. A.* **107,** 1355–1360
20. Williamson, A., Wickliffe, K. E., Mellone, B. G., Song, L., Karpen, G. H., and Rape, M. (2009) Identification of a physiological E_2 module for the human anaphase-promoting complex. *Proc. Natl. Acad. Sci. U. S. A.* **106,** 18213–18218
21. Kirkpatrick, D. S., Hathaway, N. A., Hanna, J., Elsasser, S., Rush, J., Finley, D., King, R. W., and Gygi, S. P. (2006) Quantitative analysis of in vitro ubiquitinated cyclin B1 reveals complex chain topology. *Nat. Cell Biol.* **8,** 700–710
22. Brunet, S., Maria, A. S., Guillaud, P., Dujardin, D., Kubiak, J. Z., and Maro, B. (1999) Kinetochore fibers are not involved in the formation of the first meiotic spindle in mouse oocytes, but control the exit from the first meiotic M phase. *J. Cell Biol.* **146,** 1–12
23. Sharif, B., Na, J., Lykke-Hartmann, K., McLaughlin, S. H., Laue, E., Glover, D. M., and Zernicka-Goetz, M. (2010) The chromosome passenger complex is required for fidelity of chromosome transmission and cytokinesis in meiosis of mouse oocytes. *J. Cell. Sci.* **123,** 4292–4300
24. Homer, H. A., McDougall, A., Levasseur, M., Murdoch, A. P., and Herbert, M. (2005) Mad2 is required for inhibiting securin and cyclin B degradation following spindle depolymerisation in meiosis I mouse oocytes. *Reproduction* **130,** 829–843
25. Li, M., Li, S., Yuan, J., Wang, Z. B., Sun, S. C., Schatten, H., and Sun, Q. Y. (2009) Bub3 is a spindle assembly checkpoint protein regulating chromosome segregation during mouse oocyte meiosis. *PloS One* **4,** e7701
26. Wei, L., Liang, X. W., Zhang, Q. H., Li, M., Yuan, J., Li, S., Sun, S. C., Ouyang, Y. C., Schatten, H., and Sun, Q. Y. (2010) BubR1 is a spindle assembly checkpoint protein regulating meiotic cell cycle progression of mouse oocyte. *Cell Cycle* **9,** 1112–1121
27. Schindler, K. (2011) Protein kinases and protein phosphatases that regulate meiotic maturation in mouse oocytes. *Results Probl. Cell Differ.* **53,** 309–341
28. Dupre, A., Haccard, O., and Jessus, C. (2011) Mos in the oocyte: how to use MAPK independently of growth factors and transcription to control meiotic divisions. *J. Signal Transduct.* **2011,** 350412
29. Verlhac, M. H., Lefebvre, C., Guillaud, P., Rassinier, P., and Maro, B. (2000) Asymmetric division in mouse oocytes: with or without Mos. *Curr. Biol.* **10,** 1303–1306
30. Lefebvre, C., Terret, M. E., Djiane, A., Rassinier, P., Maro, B., and Verlhac, M. H. (2002) Meiotic spindle stability depends on MAPK-interacting and spindle-stabilizing protein (MISS), a new MAPK substrate. *J. Cell Biol.* **157,** 603–613
31. Araki, K., Naito, K., Haraguchi, S., Suzuki, R., Yokoyama, M., Inoue, M., Aizawa, S., Toyoda, Y., and Sato, E. (1996) Meiotic abnormalities of c-mos knockout mouse oocytes: activation after first meiosis or entrance into third meiotic metaphase. *Biol. Reprod.* **55,** 1315–1324
32. Tong, C., Fan, H. Y., Chen, D. Y., Song, X. F., Schatten, H., and Sun, Q. Y. (2003) Effects of MEK inhibitor U0126 on meiotic progression in mouse oocytes: microtuble organization, asymmetric division and metaphase II arrest. *Cell. Res.* **13,** 375–383
33. Lin, S. L., Qi, S. T., Sun, S. C., Wang, Y. P., Schatten, H., and Sun, Q. Y. (2010) PAK1 regulates spindle microtubule organization during oocyte meiotic maturation. *Front. Biosci. (Elite Ed.)* **2,** 1254–1264
34. Sagata, N., Watanabe, N., Vande Woude, G. F., and Ikawa, Y. (1989) The c-mos proto-oncogene product is a cytostatic factor responsible for meiotic arrest in vertebrate eggs. *Nature* **342,** 512–518
35. Hashimoto, N., Watanabe, N., Furuta, Y., Tamemoto, H., Sagata, N., Yokoyama, M., Okazaki, K., Nagayoshi, M., Takeda, N., Ikawa, Y., and Aizawa, S. (1994) Parthenogenetic activation of oocytes in c-mos-deficient mice. *Nature* **370,** 68–71
36. Colledge, W. H., Carlton, M. B., Udy, G. B., and Evans, M. J. (1994) Disruption of c-mos causes parthenogenetic development of unfertilized mouse eggs. *Nature* **370,** 65–68
37. D'Avino, P. P., and Glover, D. M. (2009) Cytokinesis: mind the GAP. *Nat. Cell Biol.* **11,** 112–114
38. Willard, F. S., and Crouch, M. F. (2001) MEK, ERK, and p90RSK are present on mitotic tubulin in Swiss 3T3 cells: a role for the MAP kinase pathway in regulating mitotic exit. *Cell. Signal.* **13,** 653–664
39. Tong, C., Fan, H. Y., Lian, L., Li, S. W., Chen, D. Y., Schatten, H., and Sun, Q. Y. (2002) Polo-like kinase-1 is a pivotal regulator of microtubule assembly during mouse oocyte meiotic maturation, fertilization, and early embryonic mitosis. *Biol. Reprod.* **67,** 546–554
40. Brennan, I. M., Peters, U., Kapoor, T. M., and Straight, A. F. (2007) Polo-like kinase controls vertebrate spindle elongation and cytokinesis. *PloS One* **2,** e409
41. Santamaria, A., Neef, R., Eberspacher, U., Eis, K., Husemann, M., Mumberg, D., Prechtl, S., Schulze, V., Siemeister, G., Wortmann, L., Barr, F. A., and Nigg, E. A. (2007) Use of the novel Plk1 inhibitor ZK-thiazolidinone to elucidate functions of Plk1 in early and late stages of mitosis. *Mol. Biol. Cell.* **18,** 4024–4036
42. Wolfe, B. A., Takaki, T., Petronczki, M., and Glotzer, M. (2009) Polo-like kinase 1 directs assembly of the HsCyk-4 RhoGAP/Ect2 RhoGEF complex to initiate cleavage furrow formation. *PLoS Biol.* **7,** e1000110
43. Steegmaier, M., Hoffmann, M., Baum, A., Lenart, P., Petronczki, M., Krssak, M., Gurtler, U., Garin-Chesa, P., Lieb, S., Quant, J., Grauert, M., Adolf, G. R., Kraut, N., Peters, J. M., and Rettig, W. J. (2007) BI 2536, a potent and selective inhibitor of polo-like kinase 1, inhibits tumor growth in vivo. *Curr. Biol.* **17,** 316–322
44. Lenart, P., Petronczki, M., Steegmaier, M., Di Fiore, B., Lipp, J. J., Hoffmann, M., Rettig, W. J., Kraut, N., and Peters, J. M. (2007) The small-molecule inhibitor BI 2536 reveals novel insights into mitotic roles of polo-like kinase 1. *Curr. Biol.* **17,** 304–315
45. Berkers, C. R., Verdoes, M., Lichtman, E., Fiebiger, E., Kessler, B. M., Anderson, K. C., Ploegh, H. L., Ovaa, H., and Galardy, P. J. (2005) Activity probe for in vivo profiling of the specificity of proteasome inhibitor bortezomib. *Nat. Methods* **2,** 357–362
46. Lightcap, E. S., McCormack, T. A., Pien, C. S., Chau, V., Adams, J., and Elliott, P. J. (2000) Proteasome inhibition measurements: clinical application. *Clin. Chem.* **46,** 673–683
47. David, Y., Ziv, T., Admon, A., and Navon, A. (2010) The E2 ubiquitin-conjugating enzymes direct polyubiquitination to preferred lysines. *J. Biol. Chem.* **285,** 8595–8604
48. Elbaz, J., Reizel, Y., Nevo, N., Galiani, D., and Dekel, N. (2010) Epithelial cell transforming protein 2 (ECT2) depletion blocks

polar body extrusion and generates mouse oocytes containing two metaphase II spindles. *Endocrinology* **151,** 755–765
49. Daum, J. R., Potapova, T. A., Sivakumar, S., Daniel, J. J., Flynn, J. N., Rankin, S., and Gorbsky, G. J. (2011) Cohesion fatigue induces chromatid separation in cells delayed at metaphase. *Curr. Biol.* **21,** 1018–1024
50. Josefsberg, L. B., Galiani, D., Lazar, S., Kaufman, O., Seger, R., and Dekel, N. (2003) Maturation-promoting factor governs mitogen-activated protein kinase activation and interphase suppression during meiosis of rat oocytes. *Biol. Reprod.* **68,** 1282–1290
51. Jin, L., Williamson, A., Banerjee, S., Philipp, I., and Rape, M. (2008) Mechanism of ubiquitin-chain formation by the human anaphase-promoting complex. *Cell* **133,** 653–665
52. Panier, S., and Durocher, D. (2009) Regulatory ubiquitylation in response to DNA double-strand breaks. *DNA Repair* **8,** 436–443
53. Martinez-Forero, I., Rouzaut, A., Palazon, A., Dubrot, J., and Melero, I. (2009) Lysine 63 polyubiquitination in immunotherapy and in cancer-promoting inflammation. *Clin. Cancer Res.* **15,** 6751–6757
54. Chen, Z. J., and Sun, L. J. (2009) Nonproteolytic functions of ubiquitin in cell signaling. *Mol. Cell* **33,** 275–286
55. Erpapazoglou, Z., Dhaoui, M., Pantazopoulou, M., Giordano, F., Mari, M., Leon, S., Raposo, G., Reggiori, F., and Haguenauer-Tsapis, R. (2012) A dual role for K63-linked ubiquitin chains in multivesicular body biogenesis and cargo sorting. *Mol. Biol. Cell.* **23,** 2170–2183
56. Kravtsova-Ivantsiv, Y., and Ciechanover, A. (2012) Non-canonical ubiquitin-based signals for proteasomal degradation. *J. Cell Sci.* **125,** 539–548
57. Phu, L., Izrael-Tomasevic, A., Matsumoto, M. L., Bustos, D., Dynek, J. N., Fedorova, A. V., Bakalarski, C. E., Arnott, D., Deshayes, K., Dixit, V. M., Kelley, R. F., Vucic, D., and Kirkpatrick, D. S. (2011) Improved quantitative mass spectrometry methods for characterizing complex ubiquitin signals. *Mol. Cell. Proteomics* **10,** M110 003756
58. Ben-Saadon, R., Zaaroor, D., Ziv, T., and Ciechanover, A. (2006) The polycomb protein Ring1B generates self atypical mixed ubiquitin chains required for its in vitro histone H2A ligase activity. *Mol. Cell* **24,** 701–711
59. Mtango, N. R., Sutovsky, M., Susor, A., Zhong, Z., Latham, K. E., and Sutovsky, P. (2012) Essential role of maternal UCHL1 and UCHL3 in fertilization and preimplantation embryo development. *J. Cell. Physiol.* **227,** 1592–1603
60. Mtango, N. R., Sutovsky, M., Vandevoort, C. A., Latham, K. E., and Sutovsky, P. (2012) Essential role of ubiquitin C-terminal hydrolases UCHL1 and UCHL3 in mammalian oocyte maturation. *J. Cell. Physiol.* **227,** 2022–2029
61. Huang, X., Hatcher, R., York, J. P., and Zhang, P. (2005) Securin and separase phosphorylation act redundantly to maintain sister chromatid cohesion in mammalian cells. *Mol. Biol. Cell* **16,** 4725–4732
62. Stemmann, O., Zou, H., Gerber, S. A., Gygi, S. P., and Kirschner, M. W. (2001) Dual inhibition of sister chromatid separation at metaphase. *Cell* **107,** 715–726
63. Gorr, I. H., Boos, D., and Stemmann, O. (2005) Mutual inhibition of separase and Cdk1 by two-step complex formation. *Mol. Cell* **19,** 135–141
64. Holland, A. J., and Taylor, S. S. (2006) Cyclin-B1-mediated inhibition of excess separase is required for timely chromosome disjunction. *J. Cell Sci.* **119,** 3325–3336
65. Gorr, I. H., Reis, A., Boos, D., Wuhr, M., Madgwick, S., Jones, K. T., and Stemmann, O. (2006) Essential CDK1-inhibitory role for separase during meiosis I in vertebrate oocytes. *Nat. Cell Biol.* **8,** 1035–1037
66. Huang, X., Andreu-Vieyra, C. V., Wang, M., Cooney, A. J., Matzuk, M. M., and Zhang, P. (2009) Preimplantation mouse embryos depend on inhibitory phosphorylation of separase to prevent chromosome missegregation. *Mol. Cell. Biol.* **29,** 1498–1505
67. Chiang, T., Schultz, R. M., and Lampson, M. A. (2011) Age-dependent susceptibility of chromosome cohesion to premature separase activation in mouse oocytes. *Biol. Reprod.* **85,** 1279–1283
68. Potapova, T. A., Daum, J. R., Pittman, B. D., Hudson, J. R., Jones, T. N., Satinover, D. L., Stukenberg, P. T., and Gorbsky, G. J. (2006) The reversibility of mitotic exit in vertebrate cells. *Nature* **440,** 954–958
69. Niiya, F., Xie, X., Lee, K. S., Inoue, H., and Miki, T. (2005) Inhibition of cyclin-dependent kinase 1 induces cytokinesis without chromosome segregation in an ECT2 and MgcRacGAP-dependent manner. *J. Biol. Chem.* **280,** 36502–36509
70. Skoufias, D. A., Indorato, R. L., Lacroix, F., Panopoulos, A., and Margolis, R. L. (2007) Mitosis persists in the absence of Cdk1 activity when proteolysis or protein phosphatase activity is suppressed. *J. Cell Biol.* **179,** 671–685
71. Dumont, J., Oegema, K., and Desai, A. (2010) A kinetochore-independent mechanism drives anaphase chromosome separation during acentrosomal meiosis. *Nat. Cell Biol.* **12,** 894–901
72. Monen, J., Maddox, P. S., Hyndman, F., Oegema, K., and Desai, A. (2005) Differential role of CENP-A in the segregation of holocentric *C. elegans* chromosomes during meiosis and mitosis. *Nat. Cell Biol.* **7,** 1248–1255
73. Potapova, T. A., Daum, J. R., Byrd, K. S., and Gorbsky, G. J. (2009) Fine tuning the cell cycle: activation of the Cdk1 inhibitory phosphorylation pathway during mitotic exit. *Mol. Biol. Cell* **20,** 1737–1748
74. Petronczki, M., Glotzer, M., Kraut, N., and Peters, J. M. (2007) Polo-like kinase 1 triggers the initiation of cytokinesis in human cells by promoting recruitment of the RhoGEF Ect2 to the central spindle. *Dev. Cell.* **12,** 713–725
75. Dumont, J., and Desai, A. (2012) Acentrosomal spindle assembly and chromosome segregation during oocyte meiosis. *Trends Cell Biol.* **22,** 241–249
76. Wianny, F., Tavares, A., Evans, M. J., Glover, D. M., and Zernicka-Goetz, M. (1998) Mouse polo-like kinase 1 associates with the acentriolar spindle poles, meiotic chromosomes and spindle midzone during oocyte maturation. *Chromosoma* **107,** 430–439
77. Pahlavan, G., Polanski, Z., Kalab, P., Golsteyn, R., Nigg, E. A., and Maro, B. (2000) Characterization of polo-like kinase 1 during meiotic maturation of the mouse oocyte. *Dev. Biol.* **220,** 392–400
78. Otsuki, J., Nagai, Y., and Chiba, K. (2009) Association of spindle midzone particles with polo-like kinase 1 during meiosis in mouse and human oocytes. *Reprod. Biomed. Online* **18,** 522–528
79. Xiong, B., Yu, L. Z., Wang, Q., Ai, J. S., Yin, S., Liu, J. H., OuYang, Y. C., Hou, Y., Chen, D. Y., Zou, H., and Sun, Q. Y. (2007) Regulation of intracellular MEK1/2 translocation in mouse oocytes: cytoplasmic dynein/dynactin-mediated poleward transport and cyclin B degradation-dependent release from spindle poles. *Cell Cycle* **6,** 1521–1527
80. Gaudet, S., Langlois, M. J., Lue, R. A., Rivard, N., and Viel, A. (2011) The MEK2-binding tumor suppressor hDlg is recruited by E-cadherin to the midbody ring. *BMC Cell Biol.* **12,** 55
81. Choi, T., Fukasawa, K., Zhou, R., Tessarollo, L., Borror, K., Resau, J., and Vande Woude, G. F. (1996) The Mos/mitogen-activated protein kinase (MAPK) pathway regulates the size and degradation of the first polar body in maturing mouse oocytes. *Proc. Natl. Acad. Sci. U. S. A.* **93,** 7032–7035
82. Brunet, S., and Verlhac, M. H. (2011) Positioning to get out of meiosis: the asymmetry of division. *Human Reprod. Update* **17,** 68–75
83. Dumont, J., Million, K., Sunderland, K., Rassinier, P., Lim, H., Leader, B., and Verlhac, M. H. (2007) Formin-2 is required for spindle migration and for the late steps of cytokinesis in mouse oocytes. *Dev. Biol.* **301,** 254–265
84. Azoury, J., Lee, K. W., Georget, V., Rassinier, P., Leader, B., and Verlhac, M. H. (2008) Spindle positioning in mouse oocytes relies on a dynamic meshwork of actin filaments. *Curr. Biol.* **18,** 1514–1519
85. Weber, K. L., Sokac, A. M., Berg, J. S., Cheney, R. E., and Bement, W. M. (2004) A microtubule-binding myosin required for nuclear anchoring and spindle assembly. *Nature* **431,** 325–329
86. Wang, Y., and Riechmann, V. (2008) Microtubule anchoring by cortical actin bundles prevents streaming of the oocyte cytoplasm. *Mech. Dev.* **125,** 142–152
87. Woolner, S., O'Brien, L. L., Wiese, C., and Bement, W. M. (2008) Myosin-10 and actin filaments are essential for mitotic spindle function. *J. Cell Biol.* **182,** 77–88

Received for publication April 11, 2012.
Accepted for publication July 17, 2012.